Fragmentation of Sputtered Cluster Ions of Transition Metals: Distributions of Lifetimes and Internal Energies

ARTICLE · JANUARY 1998

DOI: 10.1007/978-3-7091-7506-4_49

6 AUTHORS, INCLUDING:

Anatoly Bekkerman

Technion - Israel Institute of Technology

41 PUBLICATIONS **273** CITATIONS

SEE PROFILE

Mikrochim. Acta [Suppl.] 15, 371–377 (1998)

Fragmentation of Sputtered Cluster Ions of Transition Metals: Distributions of Lifetimes and Internal Energies

A. D. Bekkerman[1], N. Kh. Dzhemilev[1], S. V. Verkhoturov[1], I. V. Veryovkin[1,2,*], and A. Adriaens[2]

[1] Arifov Institute of Electronics, Uzbek Academy of Sciences, 700143 Tashkent, Uzbekistan
[2] Department of Chemistry, University of Antwerp, B-2610 Antwerpen, Belgium

Abstract. Dissociation energies, lifetime distributions and internal energies have been determined experimentally for Fe_n^+ $(4 \leq n \leq 10)$ clusters produced by sputtering under 8.5 keV Xe^+ ion bombardment. The average lifetimes and the average internal energies were calculated from the experimental distributions. A comparison between the results of the present work on Ta_n^+ and Nb_n^+ clusters and those obtained earlier has been made. For all sputtered clusters compared, the linear dependence of the average internal energy $\bar{E}_{int}$ on the number of atoms, n, in the cluster has been identified. Good qualitative agreement has been found between experimental results and theoretical values determined from MD-simulations of cluster sputtering processes.

Key words: cluster sputtering, kinetic energy spectra, unimolecular fragmentation, fragmentation rate constants, lifetimes, kinetic energy release distributions, internal energy distributions.

The formation of clusters under ion bombardment of solids is one of the most interesting phenomena in ion-surface interaction physics. During the last decade, much new qualitative experimental data has been gathered on this subject [1–17]. Recent reviews of published results can be found in Refs. [18, 19]. One of the greatest difficulties in developing an adequate theoretical mechanism [20–22] for cluster formation is to compare directly such basic properties as yields, kinetic and internal energy distributions calculated for "nascent" sputtered clusters with values determined experimentally from detectable "final" clusters. This is because the high vibrational excitation of nascent clusters results in their evolution over time, the causes being the competitive processes of unimolecular fragmentation [1–8, 15] and ionisation [9–14, 16, 17].

One effective approach is to consider this problem using a combination of Molecular Dynamics (MD) and Monte Carlo (MC) computer simulations of cluster sputtering [23, 24]. Recently, very promising and realistic results for Ag_n clusters have been obtained [25] by using a so-called MD/MC-CEM interaction potential (where CEM stands for "Corrected Effective Medium") [26]. It has been shown that the nascent Ag_n clusters sputtered by sub-keV Ar^+ ions had an average internal energy of about 1 eV per constituent atom. The decomposition pathway of unstable sputtered clusters was the branching or chain decay which resulted in a total time of decomposition ranging from 10 ps to 50 ps. Such a short lifetime of evolution of Ag_n clusters was determined by their low dissociation energy and high internal energy.

Nevertheless, accurate experimental studies of the cluster emission process are the only reliable criterion for testing the theoretical model. Thus, the importance of experimental studies of a stochastic process of nascent cluster fragmentation is obvious. The fragmentation of sputtered clusters as a stochastic process has been previously investigated [27–30] and the decay rate constants and lifetime distributions of excited sputtered Ta_n^+ [27–29] and Nb_n^+ [30] clusters have been measured. It was established that within the time range of $10^{-9}-10^{-4}$ s the dependence was a

* To whom correspondence should be addressed

power function rather than an exponential one. In addition, the internal energy distributions and corresponding average internal energies were calculated by the use of Rice-Ramsperger-Kassel (RRK) theory. In contrast to the above MD/MC simulations, longer average lifetimes for Ta_n^+ and Nb_n^+ sputtered clusters were determined in the experiments and explained by their higher dissociation energy of several eV [29, 30].

In the present work the dissociation energies, the lifetime distributions and the internal energy distributions together with average values of lifetimes and internal energies were determined for Fe_n^+ ($n \leq 10$) clusters sputtered by 8.5 keV Xe^+ ions. The common regularities observed for fragmentation of the Fe_n^+, Nb_n^+ and Ta_n^+ sputtered clusters within the time range of $10^{-9}-10^{-4}$ s are considered and discussed.

Experimental

The double focusing SIMS instrument with reverse geometry employed in the present work has been described in detail previously [31]. This instrument (Fig. 1) was designed and produced as a prototype of the IMT3 ion microprobe, which was in serial production in SELMI (Sumy, Ukraine). Briefly, Xe^+ primary ions generated by a duoplasmatron ion source {1} are accelerated and mass separated in a Wien filter {3}. The focused ion beam (100 μm) bombards the sample at an angle of 45° with respect to the surface normal. The secondary ion flux is accelerated to energies, eU_0, of 2.5 keV and 5 keV and is focused by the immersion lens {8} onto the entrance slit of the magnetic mass analyser (the stigmatic magnetic prism). The energy analyser {12} is located behind the magnetic prism and consists of a three-electrode electrostatic mirror. In the sample chamber and along the entire ion flight path from the sample to the detecting system (the electron multiplier {14}), the pressure of the residual gases ($2 \cdot 10^{-8}$ Torr) was maintained by using a differential pumping system. The kinetic energy distributions of the secondary ions were determined by varying the secondary ion accelerating voltage [6].

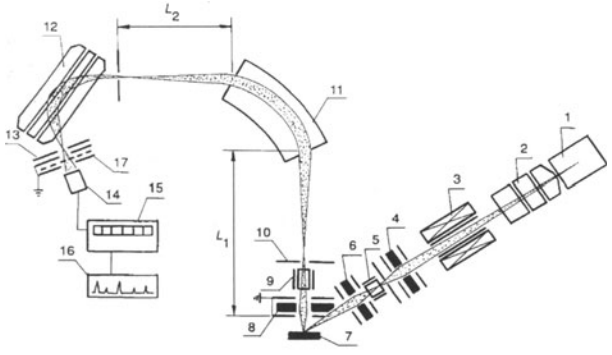

Fig. 1. Scheme of the secondary ion mass spectrometer: *1* primary ion source (duoplasmatron); *2* condenser lens; *3* Wien filter; *4* intermediate lens; *5* deflector; *6* objective lens; *7* sample; *8* immersion lens; *9* dynamic transfer system; *10* entrance slit; *11* magnetic mass analyzer; *12* electrostatic energy analyzer; *13* exit slit; *14* electron multiplier; *15* pulse counting system; *16* plotter register; *17* grid system. L_1 and L_2 are the field-free zones of the mass spectrometer

Results and Discussion

For the time range of $10^{-9}-10^{-4}$ s the fragmentation reaction identified for sputtered Fe_n^+ cluster ions ($3 \leq n \leq 10$) as well as for Nb_n^+ ($5 \leq n \leq 10$) [30] and Ta_n^+ ($4 \leq n \leq 8$) [27–29] cluster ions can be expressed as the following "quasi chemical" formula:

$$Me_n^+ \rightarrow Me_{n-1}^+ + Me \qquad (1)$$

where Me_n^+ stands for the corresponding metal clusters.

The cluster fragmentation which takes place within the accelerating electric field between the sample {7} and the accelerating electrode {8} was studied by measuring the kinetic energy distributions of *sputtered* cluster ions. For the fragmentation reactions within a time range of $\cong 10^{-8}-10^{-6}$ s, the kinetic energy of clusters gained in the accelerating field is distributed between the fragments proportionally to their masses. In this case, the cluster ion must have a kinetic energy deficit at the exit from the zone. This deficit can be determined by kinetic energy distribution measurements [6, 15]. Such distributions of Fe_n^+ secondary cluster ions are shown in Fig. 2. The extended "tails" of these distributions over the range of energies $<eU_0$ correspond to larger cluster ions (Fe_{n+1}^+) fragmented within the accelerating zone. Moreover, the cluster fragmentation times can be determined from the "tails" because different points correspond to different times [27–30].

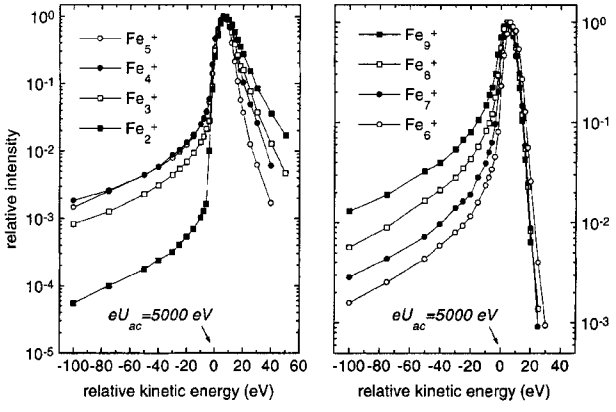

Fig. 2. Kinetic energy distributions of Fe_n^+ cluster ions ($2 \leq n \leq 9$) sputtered by 8.5 keV Xe^+ primary ions

Fragmentation within the L_2 field-free drift zone of the SIMS instrument between the mass analyser {11} and energy analyser {12} was studied by measuring the kinetic energy distributions of *fragment* ions formed by fragmentation of the sputtered clusters within the time range $\cong 5 \cdot 10^{-6} - 10^{-4}$ s. These measurements were carried out by realigning the energy analyser for the transmission of ions with energies of $eU_0 \pm 250$ eV. As seen below, such methods provide information also on the dissociation energies of the sputtered clusters.

Considered as a whole, these two ways of studying fragmentation allowed a total experimental time range of $\cong 10^{-8} - 10^{-4}$ s. In order to widen each time range, measurements were carried out for two values of the secondary accelerating voltage: $U_0 = 2.5$ kV and $U_0 = 5$ kV.

The dependence of fragmentation rate on the time immediately following cluster emission was obtained by transposing the energy scale to a time scale: $dN/dt = dN/dE \cdot dE/dt$. In this case the magnitude of *dN/dE* was determined from the kinetic energy distributions of the sputtered cluster ions using the extended "tails", as well as from the kinetic energy distributions of fragment clusters. The *dE/dt* derivative was determined from a solution of the ion movement equation for the accelerating electric field configuration. For the plane target, this electric field can be described by an approximation of a plane capacitor [15]. As seen from Fig. 3, over the entire experimental time range the dependence $F(t) = dN/dt$ can be best fitted by a power function (not by an exponential one, as might be expected):

$$F(t) = b \cdot (t + c)^{-a} \tag{2}$$

where the b parameter is given by:

$$b = N_0 \cdot (a - 1) \cdot c^{a-1} \tag{3}$$

and where N_0 is the number of fragmented clusters determined by the magnitude of the area under the curve of the *dN/dE* distribution. As usual, the a and c parameters were calculated by the least squares method (see, for instance, [27–30]). For this purpose we used the following normalised function:

$$f(t) = F(t)/N_0 \tag{4}$$

The non-exponential nature of the dependence, *F(t)*, clearly indicates the existence of clusters having different k rate constants for the fragmentation reaction. This difference is considered to be a result

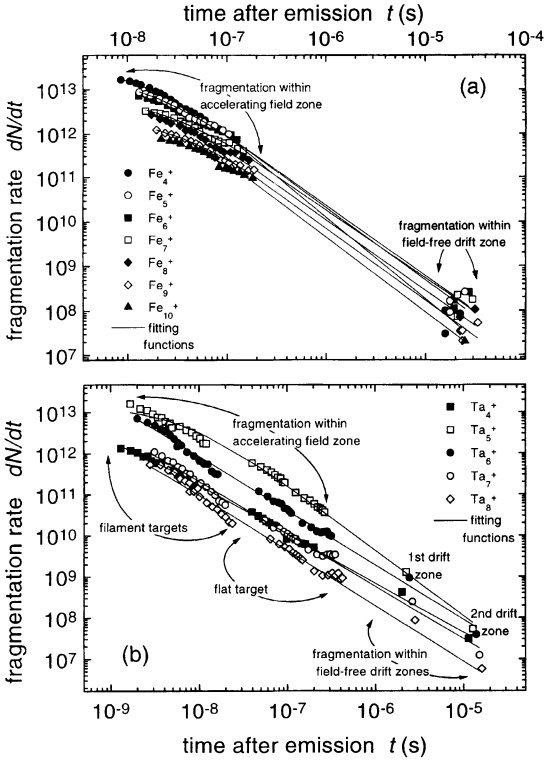

Fig. 3. Fragmentation rate dependency on the time following cluster emission for cluster ions sputtered by 8.5 keV Xe^+ ions: **a** Fe_n^+ cluster ions (the present work); **b** Ta_n^+ cluster ions (Ref. [29])

of the internal energy distribution of the sputtered clusters.

By introducing the $\varphi(k)$ distribution for the rate constants and taking into account the statistical character of the decay process of the clusters, one can consider the $f(t)$ function as a superposition of the exponential functions [28]:

$$\int_0^{k_{\max}} k \cdot \varphi(k) \exp(-tk) dk \tag{5}$$

where $k_{\max} = 10^{13}\ s^{-1}$ is the maximum rate of the decay reaction (this value is proportional to the characteristic frequency of atomic oscillations). It should be noted that, within the time range of the experiment, the $t \cdot k$ product is $\cong 10^4 - 10^9$ and the function under the integral (5) approaches zero at $k = k_{\max}$. In this case the upper limit in integral (5) can be substituted by infinity and equation (5) can be solved analytically.

The procedure described has allowed determination of the $\varphi(k)$ rate constants distributions:

$$\varphi(k) = c^{a-1} \cdot \exp(-ck) \cdot k^{a-2} / \Gamma(a - 1) \tag{6}$$

Table 1. τ average lifetimes, E_d dissociation energies (activation energies of $Me_n^+ \rightarrow Me_{n-1}^+ + Me$ fragmentation reaction) and $\bar{E}_{int}/n$ average internal energy per constituent atom determined for Ta_n^+, Nb_n^+ and Fe_n^+ clusters sputtered by Xe^+ ions

n	Ta_n^+ [29]			Nb_n^+ [30]			Fe_n^+		
	$\bar{\tau}$, s	E_d, eV	$\bar{E}_{int}/n$, eV/at	$\bar{\tau}$, s	E_d, eV	$\bar{E}_{int}/n$, eV/at	$\bar{\tau}$, s	E_d, eV	$\bar{E}_{int}/n$, eV/at
3					3.96				
4	$1.93 \cdot 10^{-9}$	6.60	1.8		2.83[a]		$1.75 \cdot 10^{-8}$	1.09	0.568
5	$1.07 \cdot 10^{-8}$	7.02	1.8	$8.68 \cdot 10^{-8}$	5.69	1.104	$2.34 \cdot 10^{-8}$	2.43	0.673
6	$0.31 \cdot 10^{-9}$	5.52	1.6	$6.18 \cdot 10^{-8}$	6.06	1.122	$3.04 \cdot 10^{-8}$	2.23	0.902
7	$0.36 \cdot 10^{-9}$	8.34	2.3	$1.71 \cdot 10^{-8}$	7.5	1.32	$4.08 \cdot 10^{-8}$	2.45	0.831
8	$0.91 \cdot 10^{-9}$			$1.29 \cdot 10^{-8}$	5.84	1.512	$3.06 \cdot 10^{-8}$	2.29	0.711
9				$2.04 \cdot 10^{-8}$	5.87	1.573	$4.65 \cdot 10^{-8}$	2.45	0.73
10				$3.69 \cdot 10^{-8}$	6.88	1.722	$5.23 \cdot 10^{-8}$	2.82	0.784
11								2.96	
12								3.2	

[a] Activation energy for $Nb_4^+ \rightarrow Nb_2^+ + Nb_2$ fragmentation.

as well as the $\Phi(\tau)$ lifetime distribution:

$$\Phi(\tau) = c^{a-1} \cdot \exp(-c/\tau) \cdot \tau^{-a}/\Gamma(a-1) \quad (7)$$

where $\tau = 1/k$ is the lifetime of the sputtered cluster. The average magnitude of the decay rate constant and the lifetime of secondary cluster ions can be determined from the distributions (6) and (7), respectively. Thus, experimental studies of the cluster fragmentation processes over a wide time range allow $\varphi(k)$ and $\Phi(\tau)$ distributions to be determined without the need for any *a priori* theoretical consideration of the process. The average lifetimes $\bar{\tau}$ of Fe_n^+ clusters are shown in Table 1 together with the corresponding values for Nb_n^+ [30] and Ta_n^+ [27–29] sputtered clusters.

The $\varphi(k)$ distribution provides information about the internal energy distribution of sputtered clusters. As shown in Ref. [28], exact knowledge of the k rate constant dependence on the $\varepsilon = E_{int}/E_d$ relative internal energy (where E_{int} is internal energy and E_d is dissociation energy) can allow the relative internal energy distribution $\Psi(\varepsilon)$ to be established. In order to estimate $\Psi(\varepsilon)$ we used the quantum version of the Rice-Ramsperger-Kassel (RRK) theory [32]. The quantum approximation of the RRK theory provides the dependence of the k rate constant on the energy of the $E_{int} = i \cdot h\nu$ vibrational excitation, taking into account the $E_d = j \cdot h\nu$ dissociation energy for the given reaction channel:

$$k = k_0 \cdot \frac{i! \cdot (i-j+s-1)!}{(i-j)! \cdot (i+s-1)!} \quad (8)$$

where $s = 3n-6$ is the number of vibrational degrees of freedom of the cluster, n is the number of atoms in it, $k_0 = 10^{13}\ s^{-1}$, $h\nu$ is a quantum of energy, ν is the average vibration frequency of the excited cluster ($\nu \cong 10^{13}\ s^{-1}$). Using Eqs. (6) and (8), one can obtain analytically the distribution of the clusters over the relative internal energies $\varepsilon = E_{int}/E_d = i/j$:

$$\Psi(\varepsilon) = \frac{(ck_0)^{a-1} j^2 (s-1)}{\Gamma(a-1)(i-j+1)(i+s)} \times \left[\frac{i!(i-j+s-1)!}{(i-j)!(i+s-1)!}\right]^{a-1} \times \exp\left[-ck_0 \frac{i!(i-j+s-1)!}{(i-j)!(i+s-1)!}\right] \quad (9)$$

For calculating the $\Psi(E_{int})$ internal energy distribution, values of the dissociation energies must be determined. The information about E_d can be obtained from the *kinetic energy release* (KER) distribution of the fragmenting clusters [33]. In the fragmentation process, this distribution characterises the part of the cluster internal energy that is expended in translational movement of fragments. The measurements of kinetic energy distributions of *fragment* cluster ions formed in the field-free zone of a mass-spectrometer allow determination of KER-distributions for the fragmenting *sputtered* clusters. In order to transform kinetic energy distributions of fragments corresponding to the laboratory reference system into KER-distributions of fragmenting clusters corresponding to the cluster centre-of-mass system, we used a data processing procedure similar to that used earlier by

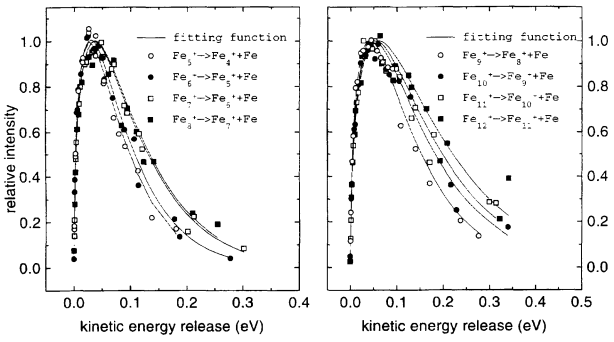

Fig. 4. Kinetic energy release distributions for the unimolecular fragmentation of Fe_n^+ cluster ions ($5 \leq n \leq 12$) within field-free zone (L_2) of the mass spectrometer

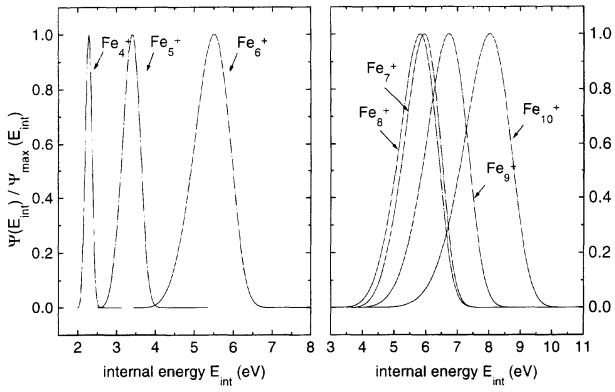

Fig. 5. Internal energy distributions of Fe_n^+ cluster ions ($4 \leq n \leq 10$) sputtered by 8.5 keV Xe^+ primary ions

various authors [34, 35] (for details, see Ref. [33]). KER-distributions of Fe_n^+ clusters are shown in Fig. 4. The dissociation energy (the activation energy for a given cluster decay channel) can be determined within the framework of a so-called "evaporation ensemble" conception [36–38]. Then the KER-distribution of fragment ions is described by the following expression.

$$dN/dE \propto E^l \exp(-E/k_B T^{\#}) \qquad (10)$$

where E is the kinetic energy of the fragment, k_B is Boltzman's constant, $T^{\#}$ is the temperature of the excited cluster (this temperature corresponds to the excitation energy per degree of freedom). As before, we obtained l and $T^{\#}$ parameters using the least squares method for approximating the experimental KER-distributions by expression (10). The relationship between the dissociation energy E_d and the temperature $T^{\#}$ is described in terms of the "evaporative ensemble" conception by the following expression:

$$E_d = \frac{\gamma(n) \cdot k_B T^{\#}}{1 - \gamma(n)/2C(n) + [\gamma(n)/C(n)]^2/12 + \ldots} \qquad (11)$$

where $\gamma(n)$ is the Gspann's parameter dependent on the cluster size n and $C(n)$ is the heat capacity expressed in units of k_B. In our case $\gamma(n) \approx 22.6 \pm 0.4$.

The E_d dissociation energies calculated for Fe_n^+ as well as for Nb_n^+ [30] and Ta_n^+ [29] sputtered clusters are shown in Table 1. The reliability of the procedure was first tested on sputtered Nb_n^+ clusters ($3 \leq n \leq 10$) [30]. Generally, values of the dissociation energy of the sputtered Nb_n^+ clusters were in agreement

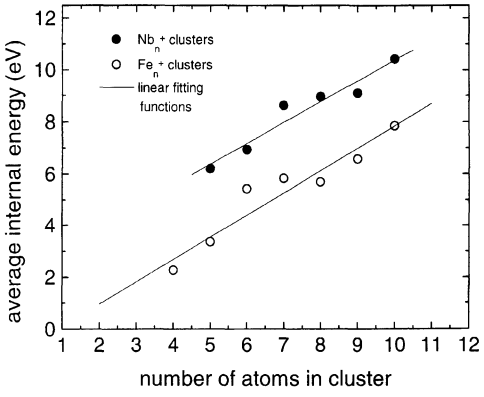

Fig. 6. Dependency of the average internal energy of Fe_n^+ and Nb_n^+ [30] sputtered clusters on the number of atoms in the cluster

($\cong 10\%$) with the data obtained in the experiments on collision-induced cluster dissociation [39, 40].

Internal energy distributions of Fe_n^+ clusters ($4 \leq n \leq 10$) are shown in Fig. 5. The $\bar{E}_{\text{int}}/n$ average internal energies (per constituent atom) calculated from the internal energy distribution are shown in Table 1 together with the corresponding values for Nb_n^+ [30] and Ta_n^+ [29] clusters. In Fig. 6, the dependency of $\bar{E}_{\text{int}}$ on the number of atoms in the cluster is shown for Nb_n^+ [30] and Fe_n^+ sputtered clusters. As seen from the plots and Table 1, the dependency is a linear one and the $\bar{E}_{\text{int}}/n$ values depend weakly on cluster size, being approximately equal to 1.88 eV/at, 1.39 eV/at and 0.75 eV/at for Ta, Nb and Fe, respectively. A similar result was obtained by the MD simulation of the sputtering processes [23, 25]. The data in Ref. [23, 25] were used on nascent clusters of Ag_n ($n \leq 31$) sputtered by keV and sub-keV

Ar^+ ions. In the simulations, these neutral clusters were considered immediately after the moment of emission. The $\bar{E}_{int}/n$ values for Ag_n clusters were found to be 1.5 eV/at, approximately. In contrast to the MD/MC simulation which demonstrates the branching or chain decay characterised by a decomposition time of $10^{-11}-5\cdot10^{-11}$ s, it has been shown [29, 30] that the possibility of rapid chain decay is very questionable for Ta_n^+ and Nb_n^+ charged sputtered clusters because their dissociation energies are approximately twice as large as those of Ag clusters [25]. In this case, the internal energy of small Ta_n^+ and Nb_n^+ nascent clusters may be insufficient for a further chain of decay if both the ionisation act and the first decay event have taken place already. Such a time evolution of Ta_n and Nb_n clusters is considerably different from that described earlier [23, 25] but the dependence of $\bar{E}_{int}$ on cluster size is in qualitative agreement with the data of Ref. [23, 25]. The higher $\bar{E}_{int}/n$ average internal energies of Ta_n^+ cluster ions compared with Nb_n^+ clusters may be explained by the differences in time range of the fragmentation studies [15, 28, 29] and the influence of the time range on the experimental results of the sputtered cluster fragmentation study will be considered in detail in a following paper.

In contrast to the results obtained for Ta_n^+ and Nb_n^+ cluster ions, those for Fe_n^+ clusters demonstrate a very good agreement with the results of the MD/MC simulation in Ref. [25]. This is because the dissociation energies of Fe_n^+ cluster ions (see Table 1) are of the same order as those for Ag_n clusters. The similarity allows us to suppose that the time evolution of the nascent Fe_n clusters can be accurately simulated using the MD/MC-CEM interaction potential. In this connection, the agreement between experimental values of $\bar{E}_{int}/n$ for Fe_n^+ cluster ions and those predicted theoretically in Ref. [25] for "final" Ag_n neutral clusters should be noted. For the Fe_n^+ cluster ions, comparison between our experimental results and the MD/MC simulations allow us to suggest the possibility of chain decay steps in cluster time evolution.

In spite of the experimental limitations of $5\cdot10^{-10}-10^{-9}$ s for the achievable time range of direct observations of the sputtered cluster fragmentation, the methods to study this stochastic process developed in Refs. [29, 30] and used in the present work can be extrapolated to shorter fragmentation times. The procedure is to consider the sputtered cluster time evolution as well as the cluster internal energy filtering taking place in the instruments. This approach will be presented in our next paper referred to above.

Conclusion

At the moment, it seems possible that there is some agreement regarding the process of sputtered cluster time evolution. This includes the emission of vibrationally excited nascent clusters that are transformed into experimentally detectable final cluster ions in the processes of ionisation and fragmentation. This is why modern theoretical and experimental approaches to study this process demonstrate a good agreement when results are compared. In summary, future developments in the study of cluster emission during sputtering must include a close interaction between experimental work on cluster fragmentation and theoretical MD/MC simulation of cluster emission and time evolution. One can expect that this will result in a realistic physical explanation of the phenomena.

Acknowledgements. The authors would like to acknowledge the support from INTAS (Project 96-0470). Two of the authors would also like to thank Belgian organisations IUAP and DWTC (I. V. Veryovkin) and FWO (A. Adriaens) for providing an opportunity to conduct this study.

References

[1] W. Ens, R. Beavis, K. G. Standing, *Phys. Rev. Lett.* **1983**, *50*, 27.
[2] N. Kh. Dzhemilev, S. V. Verkhoturov, *Izv. Akad. Nauk SSSR Ser. Fiz.* **1985**, *49*, 1831.
[3] I. Katakuze, T. Ichihara, Y. Fujita, T. Matsuo, T. Sakurai, H. Matsuda, *Int. J. Mass Spectrom. Ion Proc.* **1985**, *67*, 229.
[4] W. Begemann, K. H. Meiwes-Broer, H. O. Lutz, *Phys. Rev. Lett.* **1985**, *56*, 2248.
[5] N. Kh. Dzhemilev, S. V. Verkhoturov, U. Kh. Rasulev, *Nucl. Instr. Meth.* **1987**, *B29*, 531.
[6] N. Kh. Dzhemilev, S. V. Verkhoturov, I. V. Veriovkin, *Nucl. Instr. Meth.* **1990**, *B51*, 219.
[7] I. Katakuze, H. Ito, T. Ichihara, *Int. J. Mass Spectrum. Ion Proc.* **1990**, *97*, 47.
[8] W. Begemann, K. H. Meiwes-Broer, H. O. Lutz, *J. Phys. (Paris)* **1989**, *50*, 133.
[9] H. Gnaser, W. O. Hofer, *Appl. Phys.* **1989**, *A48*, 261.
[10] H. Oechner, *Int. J. Mass Spectrom. Ion Proc.* **1990**, *103*, 31.
[11] B. N. Makarenko, A. B. Popov, A. A. Shaporenko, A. P. Shergin, *Rad. Eff. Def. Solids* **1991**, *116*, 15.
[12] S. R. Coon, W. F. Calaway, J. W. Burnett, M. J. Pellin, D. M. Gruen, D. R. Spiegel, J. M. White, *Surf. Sci.* **1991**, *259*, 275.
[13] S. R. Coon, W. F. Calaway, M. J. Pellin, G. A. Curlec, J. M. White, *Nucl. Instr. Meth.* **1993**, *B82*, 329.

[14] A. Wucher, M. Wahl, H. Oechner, *Nucl. Instr. Meth.* **1993**, *B82*, 337.
[15] N. Kh. Dzhemilev, A. M. Goldenberg, I. V. Veriovkin, S. V. Verkhoturov, *Int. J. Mass Spectrom. Ion Proc.* **1991**, *107*, R19.
[16] A. Wucher, M. Wahl, in: *Secondary Ion Mass Spectrometry SIMS XI* (A. Bennighoven, H. W. Werner, B. Hegenhoff, eds.) Wiley, Chichester, 1997, p. 65.
[17] A. Wucher, M. Wahl, *Nucl. Instr. Meth.* **1996**, *B115*, 581.
[18] H. M. Urbassek, W. O. Hofer, *K. Danske Vidensk Selsk. Mat. Fys. Medd.* **1993**, *43*, 97.
[19] W. O. Hofer, in: *Sputtering by Particle Bombardment, Vol. 3* (R. Behrish, K. Wittmaack, eds.) Springer, Berlin Heidelberg New York Tokyo, 1991.
[20] H. M. Urbassek, *Rad. Eff. Def. Solids* **1989**, *109*, 293.
[21] I. S. Bitensky, E. S. Parilis, *Nucl. Instr. Meth.* **1987**, *B21*, 26.
[22] B. V. King, I. S. T. Tsong, S. H. Lin, *Int. J. Mass Spectrom. Ion Proc.* **1987**, *78*, 341.
[23] A. Wucher, B. J. Garrison, *Phys. Rev.* **1992**, *B46*, 4885.
[24] A. Wucher, *Nucl. Instr. Meth.* **1993**, *B83*, 79.
[25] A. Wucher, B. J. Garrison, *J. Chem. Phys.* **1996**, *105*(14), 5999.
[26] C. L. Kelchner, D. M. Halstead, L. S. Perkins, N. M. Wallace, A. E. DePristo, *Surf. Sci.* **1994**, *310*, 425.
[27] N. Kh. Dzhemilev, I. V. Veriovkin, S. V. Verkhoturov, A. M. Goldenberg, *Izv. Akad. Nauk SSSR Ser. Fiz.* **1991**, *55*, 2418.
[28] N. Kh. Dzhemilev, A. M. Goldenberg, I. V. Veriovkin, S. V. Verkhoturov, *Int. J. Mass Spectrom. Ion Proc.* **1995**, *141*, 209.
[29] N. Kh. Dzhemilev, A. M. Goldenberg, I. V. Veriovkin, S. V. Verkhoturov. *Nucl. Instr. Meth.* **1996**, *B114*, 245.
[30] I. V. Veryovkin, S. V. Verkhoturov, A. M. Goldenberg, N. Kh. Dzhemilev, *Izv. Akad, Nauk Ser. Fiz.*, **1994**, *58(10)*, 63 and *Bull. Russ. Acad. Sci.–Phys.* **1994**, *58(10)*, 1635.
[31] A. D. Bekkerman, N. Kh. Dzhemilev, V. M. Rotstein, *Surf. Interf. Anal.* **1990**, *15*, 587.
[32] P. J. Robinson, K. A. Holbrook, *Unimolecular Reactions*, Wiley, London, 1972.
[33] I. V. Veryovkin, S. V. Verkhoturov, A. M. Goldeberg and N. Kh. Dzhemilev, *Izv. Akad. Nauk Ser. Fiz.* **1994**, *58(3)*, 56 and *Bull. Russ. Acad. Sci.–Phys.* **1994**, *58(3)*, 416.
[34] M. F. Jarrold, A. J. Illies, N. J. Kirchner, W. Wagner-Redeker, M. T. Bowers, M. L. Mandich, J. L. Beauchamp, *J. Phys. Chem.* **1983**, *87*, 2213.
[35] P. P. Radi, M. E. Rincon, M. T. Hsu, J. Brodbelt-Lustig, P. Kemper, M. T. Bowers, *J. Phys. Chem.* **1989**, *93*, 6187.
[36] C. E. Klots, *Int. J. Mass Spectrom. Ion Proc.* **1990**, *100*, 457.
[37] C. E. Klots, *Z. Phys.* **1991**, *D20*, 105.
[38] C. E. Klots, *Z. Phys.* **1991**, *D21*, 335.
[39] D. A. Hales, L. Lian, P. B. Armentrout, *Int. J. Mass Spectrom. Ion Proc.* **1990**, *102*, 269.
[40] S. K. Loh. D. A. Hales, Li Lian, P. B. Atmentrout, *J. Chem. Phys.* **1989**, *90(10)*, 5466.